Liraglutide Attenuates Hepatocyte Ferroptosis in an In Vitro Model of Metabolic Dysfunction-Associated Steatotic Liver Disease

Jing BAI[1], Yanxin XIAO[3], Pingping LOU[2], Jie ZHANG[2], Yan LIU[2], Yaru ZHOU[2]

[1]Department of Endocrinology, Cangzhou People's Hospital, Cangzhou, Hebei, China, [2]Department of Endocrinology, The Third Hospital of Hebei Medical University, Shijiazhuang, Hebei, China, [3]Department of Endocrinology, Baoding NO. 1 Central Hospital, Baoding, Hebei, China

Received January 16, 2026
Accepted June 9, 2026

Summary

This study examined the potential of liraglutide to attenuate ferroptosis in an *in vitro* model of metabolic dysfunction-associated steatotic liver disease (MASLD). HepG2 cells were allocated into three groups: control (Con), free fatty acid (FFA)-treated, and FFA with liraglutide treatment (FFA+LI). After 48 h of treatment, intracellular triglyceride (TG), glutathione (GSH), malondialdehyde (MDA), and iron levels were quantified using commercially available kits. Superoxide dismutase (SOD) activity was also measured. Lipid accumulation was visualized *via* Oil Red O staining. Expression of ferroptosis-associated genes was assessed through quantitative RT-PCR and western blotting. FFA treatment induced significant lipid accumulation, elevated TG, MDA, and iron levels, and reduced SOD activity and GSH levels compared to the Con group (all $p<0.05$). Additionally, FFA exposure increased the expression of *TFR1* and downregulated *SLC7A11*, *NRF2*, and *GPX4* ($p<0.05$ for all comparisons vs. Con). Liraglutide treatment partially reversed these changes, as evidenced by reduced MDA levels and iron content, downregulation of *TFR1*, and upregulation of *NRF2* and *GPX4* (FFA+LI vs. FFA, all $p<0.05$). Liraglutide demonstrated the ability to mitigate lipid accumulation, oxidative stress, and iron overload in HepG2 cells subjected to FFA-induced injury. These effects were associated with modulation of ferroptosis-related gene expression, suggesting a mechanistic basis for the potential protective role of liraglutide in MASLD.

Key words

Ferroptosis • Free fatty acid • Liraglutide • Metabolic dysfunction-associated steatotic liver disease • Oxidative stress

Corresponding author

Y. Zhou, Department of Endocrinology, The Third Hospital of Hebei Medical University, Ziqiang Road 139, Shijiazhuang 050051, Hebei, China. E-mail: zyrydsy@hebmu.edu.cn

Introduction

Metabolic dysfunction-associated steatotic liver disease (MASLD) is characterized by excessive hepatic fat accumulation attributable to nonalcoholic and nonviral etiologies and represents a significant risk factor for irreversible conditions, including insulin resistance, diabetes mellitus, and liver cirrhosis [1]. The global prevalence of MASLD is estimated to be approximately 25.24 %, with a significantly higher prevalence of about 52.27 % reported among overweight or obese populations in Asia [2,3].

The imbalance of oxidative stress and related lipid peroxidation play a key role in MASLD [3]. Ferroptosis is a recently characterized form of programmed cell death driven by intracellular iron overload, resulting in oxidative stress and lipid peroxidation [4]. Significant evidence has indicated that ferroptosis plays a key role in the pathogenesis of MASLD [5]. When the expression of GPX4 and GSH anti-oxidative stress proteins is decreased, and the activity of SOD is decreased, the level of cellular lipid peroxidation and MDA will increase, leading to the death of hepatocytes [6]. SLC7A11 plays an important role in cellular anti-oxidation. The decrease of its expression will lead to the decrease of cellular antioxidant capacity and the increase of lipid peroxidation [7]. Nrf2 is one of the

 An open access article under the CC BY 4.0 license https://creativecommons.org/licenses/by/4.0/ © 2026 by the authors. Published by the Institute of Physiology, Czech Academy of Sciences, Prague, Czech Republic. E-mail: physres@fgu.cas.cz, www.biomed.cas.cz/physiolres

regulators of intracellular redox homeostasis and inhibits the occurrence and progression of ferroptosis by reducing the level of intracellular oxidative stress [8]. Patients with MASLD demonstrate hepatic iron accumulation, and the use of iron chelators improves liver pathological changes associated with MASLD [9].

Liraglutide, a glucagon-like peptide-1 receptor agonist, has been reported to ameliorate MASLD in both human and animal studies by reducing hepatic steatosis, inflammation, and fibrosis, as well as by improving insulin sensitivity and oxidative stress markers [10,11]. *In vitro*, liraglutide has been observed to reduce lipid content in hepatocytes exposed to free fatty acids (FFA), thereby decreasing oxidative stress and limiting the progression of steatosis [12]. Also, as a hypoglycemic agent, liraglutide has demonstrated efficacy in alleviating ferroptosis in liver tissue of diabetic models [13,14]. However, the effect of liraglutide on ferroptosis in an *in vitro* model of MASLD remains largely unexplored.

Therefore, this study aimed to examine the role of liraglutide in modulating ferroptosis in palmitic acid/oleic acid (PA/OA)-treated HepG2 cells, whether liraglutide exerts beneficial effects by inhibiting ferroptosis, thereby providing more direct evidence of its effects on MASLD.

Methods

Cell culture

Human hepatocytes (HepG2) were purchased from Shanghai Zhong Qiao Xin Zhou Biotechnology Co., Ltd (SFM0022). Cells were seeded in 6-well plates at a density of 2×10^4 cells/cm^2 (approximately 4×10^5 cells/well in 6-well plates; corresponding densities were used for other plate formats) and cultured in Minimum Essential Medium (MEM) supplemented with 10 % fetal bovine serum (FBS) and 1 % penicillin-streptomycin at 37 °C in a humidified atmosphere containing 5 % CO_2. Upon reaching 80 % confluence, cells were subjected to the following experiments. Collagen coating was not used for any culture vessels. To determine the optimal concentrations of free fatty acids (FFAs) and liraglutide, cells were exposed to varying concentrations of FFAs (Cat: KT003-004, Xi'an Kunchuang Technology Co., Ltd., China) with an OA:PA ratios of 2:1 (0, 50/25, 100/50, 200/100, 300/150, and 400/200 μM) and liraglutide (Novo Nordisk, Denmark) at concentrations of 0, 50, 100, 200, 300, and 500 nmol/l for 24 or 48 h. Cell viability was assessed using the MTT assay. Based on the MTT results, 200 μM PA and 100 μM OA were selected for steatosis induction, and 100 nM liraglutide was selected for subsequent experiments. For FFA preparation, palmitic acid (200 μM) and oleic acid (100 μM) were complexed with 10 % fatty acid-free bovine serum albumin (BSA) at a 5:1 molar ratio (FFA:BSA) at 37 °C for 1 h before dilution in complete culture medium. The final BSA concentration in the working medium was approximately 0.67 % (w/v). This conjugation method is based on established protocols for FFA-induced lipotoxicity in hepatocyte models. For steatosis induction, HepG2 cells were treated with FFAs (200 μM PA/100 μM OA) for 24 h. During steatosis induction, the culture medium consisted of MEM supplemented with 10 % FBS, containing 0.67 % BSA (from the FFA-BSA complex) and the indicated concentrations of FFAs. The 10 % FBS concentration remained constant throughout all experimental conditions. Steatosis induction was confirmed by Oil Red O staining and elevated triglyceride levels. After FFA treatment, cells were co-treated with or without liraglutide for an additional 24 h according to the experimental design. Cells were allocated into the following three groups: (1) Control group (Con): cultured in MEM supplemented with 10 % FBS and vehicle (BSA + ethanol); (2) Free fatty acid-treated group (FFA): cultured in medium containing 200 μM PA and 100 μM OA; (3) Free fatty acid + liraglutide treatment group (FFA+LI): cultured in medium containing 200 μM PA, 100 μM OA, and 100 nM liraglutide.

MTT assay for cell viability

HepG2 cells were cultured in 96-well plates at a density of 1×10^4 cells/well. Following treatment, 20 μl of MTT stock solution (Cat: G020-1-1; Nanjing Jiancheng Bioengineering Institute, China) was added to each well. Cells were incubated at 37 °C for 4 h. The medium was subsequently removed, and dimethyl sulfoxide was added to dissolve the formazan crystals. Absorbance was measured at 490 nm using a microplate reader to assess cell viability.

Oil red O staining

Lipid droplets were visualized and quantified using an Oil Red O (ORO) staining kit (Cat: G1262; Beijing Solarbio Science & Technology Co., Ltd, China), following the manufacturer's instructions. Briefly, cells were fixed with ORO fixative for 20 min and stained with freshly prepared ORO staining solution for an additional 20 min. After washing with 60 % isopropanol, cells were counterstained with Mayer's hematoxylin for 2 min.

Lipid droplets were then observed and imaged using a microscope.

TG measurement

Intracellular triglyceride (TG) levels were measured using a reagent kit (Cat: A110-1-1; Nanjing Jiancheng Bioengineering Institute, China), following the manufacturer's instructions. Assay reagents were prepared accordingly. Cells were lysed in lysis buffer, and the lysates were centrifuged to collect the supernatant. The supernatant was then mixed with the working solution and incubated at 37 °C for 10 min. Absorbance was measured at 500 nm, and TG concentrations were calculated.

GSH level, SOD activity and MDA content measurement

The levels of glutathione (GSH), superoxide dismutase (SOD) activity, and malondialdehyde (MDA) content in cells were measured using commercial assay kits, following the manufacturer's protocols (Cat: G0206F, G0101F, G0109F; Suzhou Grace Biotechnology Co., Ltd, China).

Iron content measurement

Intracellular iron concentration was measured using an Iron Assay Kit (Cat: G1212F; Suzhou Grace Biotechnology Co., Ltd, China), following the manufacturer's instructions. Under acidic conditions, iron dissociates from the complex and is then reduced to divalent iron by reducing agents, which reacts with ferrozine to form a purplish red product. It has characteristic absorption peak at 562 nm in microplate reader, and the iron content can be calculated by measuring the absorbance. Briefly, cells were lysed on ice, and the supernatants were collected after centrifugation at 3,000 rpm for 10 min. The supernatants were then incubated with 520 µl of Reagent 1 and 40 µl of Reagent 2 at 37 °C for 15 min. Absorbance was measured at 562 nm using a microplate reader.

Real-Time PCR

Total RNA was extracted from cells using TRIzol reagent. Complementary DNA (cDNA) synthesis was performed using the GoScript Reverse Transcription System (Promega, USA) according to the manufacturer's instructions. Quantitative gene expression was assessed by real-time PCR using the CFX96 Touch Deep Well Real-Time PCR Detection System (BIO-RAD, USA). Target genes were amplified with the primers listed in Table 1, and β-actin was used as an endogenous control. Each 20 µl reaction mixture consisted of 10 µl of 2× GoTaq qPCR Master Mix (Promega, USA), 2 µl of cDNA, 0.8 µl of PCR primers, and nuclease-free water. All reactions were performed in triplicate. Gene expression levels were normalized to β-actin, and the $2^{-\Delta\Delta Ct}$ method was used for quantitative analysis.

Table 1. The sequences of the primers.

Gene	**Forward primer**	**Reverse primer**
SLC7A11	5'-GTCCTTTCAAGGTGCCACTG-3'	5'-GTGATGACGAAGCCAATCCC-3'
GPX4	5'-ATACGCTGAGTGTGGTTTGC-3'	5'-GCGGCGAACTCTTTGATCTC-3'
Nrf2	5'-GCGACGGAAAGAGTATGAGC-3'	5'-GGGCAACCTGGGAGTAGTT-3'
TFR1	5'-GGTGTAGTGGAAGTATCTGCTATGG-3'	5'-GAAGTCCTCTCCTGGCTCCTC-3'

SLC7A11, solute carrier family 7 member 11; GPX4, glutathione peroxidase 4; Nrf2, nuclear factor erythroid-2-related factor 2; TFR1, transferrin receptor 1.

Western blot

Proteins were extracted using RIPA lysis buffer supplemented with protease inhibitors (NCM Biotech, China). Total protein lysates were used for all Western blot analyses, including NRF2 detection. Protein concentrations were determined using the BCA Protein Assay Kit (Biological Industries, Israel). Equal amounts of protein were separated by 10 % SDS-polyacrylamide gel electrophoresis and transferred onto PVDF membranes. Membranes were blocked for 1 h using a solution containing 0.1 % Tween-20 and 5 % bovine serum albumin in TBS, followed by overnight incubation at 4 °C with specific primary antibodies against SLC7A11 (1:1000, 26864-1-AP, Proteintech, Wuhan, China), Nrf2 (1:5000, 16396-1-AP, Proteintech, Wuhan, China), GPX4 (1:1000, 14432-1-AP, Proteintech, Wuhan, China), TFR1 (1:5000, 10084-2-AP, Proteintech, Wuhan, China), and β-actin (1:20000, 66009-1-Ig, Proteintech, Wuhan, China).

Subsequently, membranes were incubated with Dylight800-conjugated secondary antibodies (goat anti-rabbit or anti-mouse IgG, 1:7000, A23910, Abbkine Scientific, Wuhan, China) at 37 °C for 2 h. Protein bands were visualized using the Odyssey fluorescence imaging system, and densitometric analysis was performed using ImageJ software. β-actin was used as an internal control. All Western blot experiments were independently repeated three times (n=3), and data are presented as mean ± SD.

Statistical analysis

Statistical analysis was conducted using SPSS version 22.0. All experiments were performed in triplicate (technical replicates). Data are presented as mean ± standard deviation. Differences between the two groups were assessed using the Student's *t*-test, while one-way analysis of variance was used for comparisons among three groups. Following one-way analysis of variance, *post hoc* comparisons among the three experimental groups were conducted using Tukey's honestly significant difference (HSD) test (when equal variances were assumed) or the Games-Howell test (when equal variances were not assumed). A value of $p<0.05$ was considered statistically significant.

Results

Effects of different concentrations of palmitic/oleic acid and liraglutide on the viability of HepG2 cells

Cell viability was significantly reduced following treatment with 300/150 μM palmitic/oleic acid at both 24 and 48 h ($p<0.05$), as well as with liraglutide concentrations starting from 200 nmol/l at both time points when compared to the Con group ($p<0.05$). From these findings, treatment with 200/100 μM palmitic/oleic acid and 100 nmol/l liraglutide for 24 h was selected for subsequent experiments (Fig. 1A, B).

Liraglutide alleviated lipid accumulation caused by palmitic/oleic acid

Compared with the Con group, FFA treatment resulted in noticeable lipid accumulation (Fig. 2A) and a significant increase in intracellular TG levels ($p<0.05$; FFA vs. Con) (Fig. 2B). Treatment with liraglutide attenuated both lipid accumulation and TG levels induced by FFA ($p<0.05$; FFA+LI vs. FFA), indicating that liraglutide effectively reduced lipid accumulation caused by palmitic/oleic acid (Fig. 2A, B).

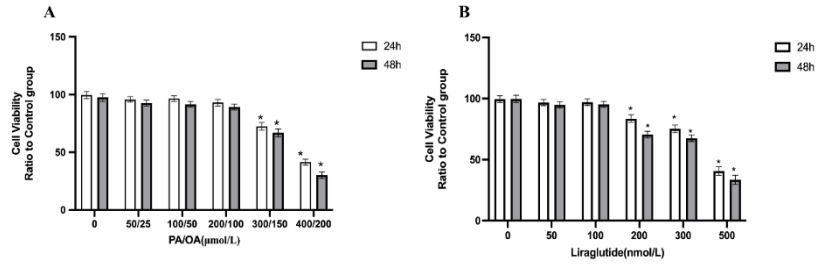


Fig 1. The effect of different concentrations of PA/OA and liraglutide on HepG2 cells. Cells were treated with different concentrations. Data represent the mean ± SD of three independent experiments (n=3). Compared with control group, * $p<0.05$, ** $p<0.01$, *** $p<0.001$, **** $p<0.0001$.

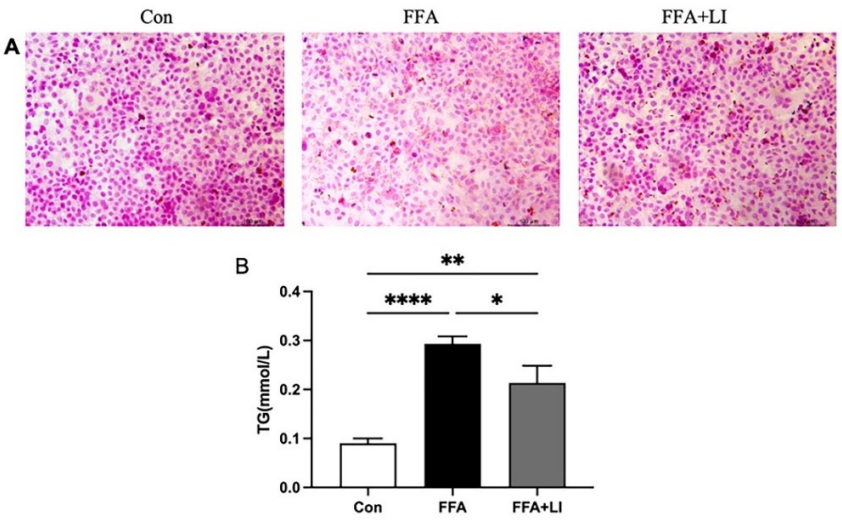


Fig 2. The effects of liraglutide on lipid metabolism. Liraglutide treatment significantly reduced lipid content (**A**) and triglyceride content (**B**) caused by PA/OA in HepG2 cells. Data represent the mean ± SD of three independent experiments (n=3). Compared with control group, * $p<0.05$, ** $p<0.01$, *** $p<0.001$, **** $p<0.0001$.

Liraglutide improved oxidative stress induced by palmitic/oleic acid

SOD activity and GSH levels were significantly decreased, while MDA levels were significantly increased in HepG2 cells treated with FFA (p<0.05 for all; FFA vs. Con), indicating that FFA treatment induced oxidative stress in hepatocytes when compared to the Con group. These changes were partially reversed by liraglutide treatment, as evidenced by improved SOD activity and GSH levels, along with reduced MDA levels (p<0.05 for all; FFA+LI vs. FFA), indicating that liraglutide mitigated oxidative stress and lipid peroxidation (Fig. 3A, B, and C).

Liraglutide reduced iron overload induced by palmitic /oleic acid

When compared to the Con group, FFA treatment significantly increased intracellular iron content in HepG2 cells (p<0.05; FFA vs. Con), indicating that FFA induced iron overload in hepatocytes. This iron accumulation was partially alleviated by liraglutide treatment (p<0.05; FFA+LI vs. FFA), suggesting that liraglutide attenuated intracellular iron overload (Fig. 4).

The effect of liraglutide on ferroptosis-related genes expressions

As shown in Figure 5A, FFA treatment significantly downregulated *SLC7A11* mRNA expression compared to the Con group (p<0.05). Additionally, *TFR1* mRNA expression was significantly increased, while *NRF2* and *GPX4* mRNA expression were significantly decreased in the FFA-treated group (p<0.05 for all; FFA vs. Con). Upregulation of *TFR1* suggests enhanced cellular iron uptake capacity, a key step in initiating ferroptosis. Conversely, downregulation of *NRF2* and its target GPX4 indicates impaired antioxidant defense, which increases susceptibility to lipid peroxidation and ferroptosis.

As shown in Figure 5B, densitometric analysis (normalized to β-actin, which was consistent across all groups) confirmed that FFA treatment decreased *GPX4* and *NRF2* protein expression while increasing *TFR1* expression compared to the Con group. These changes were partially reversed by liraglutide treatment, except for *SLC7A11*, which did not show a significant change at the protein level (p>0.05; FFA+LI vs. FFA). Taken together, these findings suggest that liraglutide may mitigate FFA-induced ferroptosis in HepG2 cells by promoting an anti-ferroptotic gene expression profile (Fig. 5A and 5B).

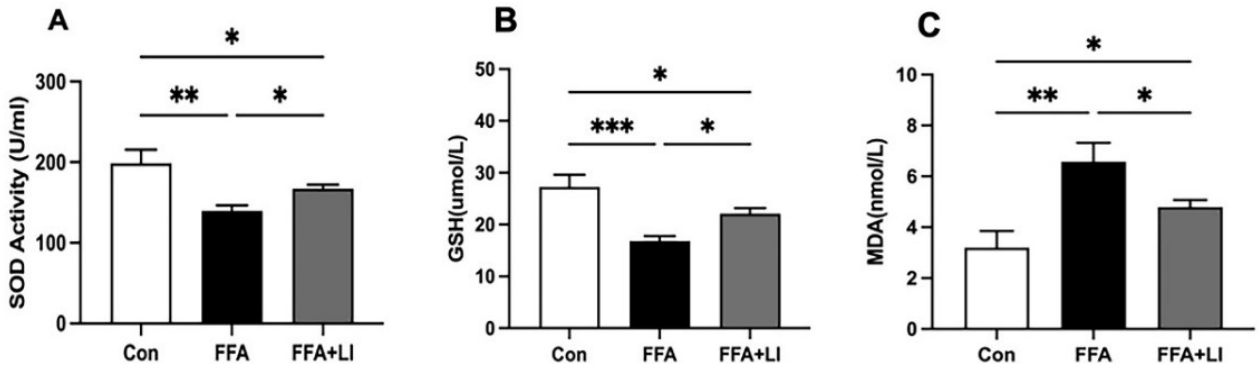


Fig 3. The effect of liraglutide on cell oxidative stress. Liraglutide improved the anti-oxidative stress ability of HepG2 cells induced by PA/OA and reduced lipid peroxidation. Data represent the mean ± SD of three independent experiments (n=3). Compared with control group, * p<0.05, ** p<0.01, *** p<0.001.

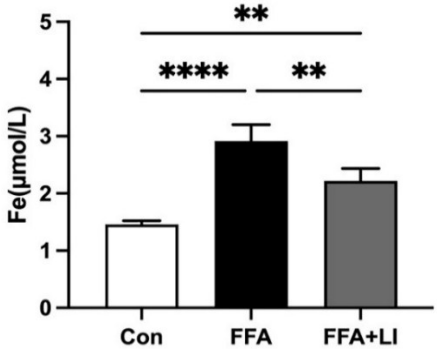


Fig. 4. Liraglutide reduced iron overload. Liraglutide reduced iron overload in HepG2 cells induced by PA/OA. Data represent the mean ± SD of three independent experiments (n=3). Compared with control group, ** p<0.01, *** p<0.001.

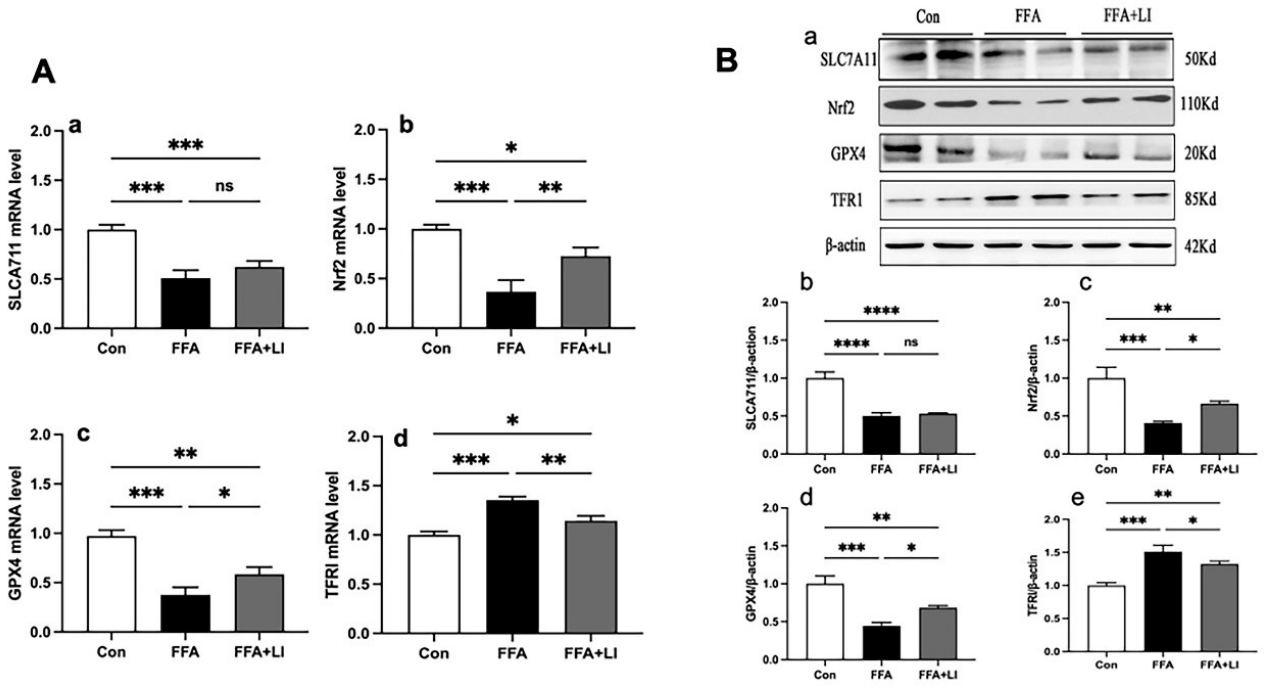


Fig 5. The effects of liraglutide on ferroptosis-related gene expression. FFA treatment caused significantly decreased Nrf2 and GPX4 expression, while increased TFR1at mRNA (**A**) and protein levels (**B**), and liraglutide treatment could improve FFA-induced ferroptosis in HepG2 cells by promoting an anti-ferroptotic gene profile. Data represent the mean ± SD of three independent experiments (n=3). Compared with control group, * $p<0.05$, ** $p<0.01$, *** $p<0.001$, **** $p<0.0001$, ns ($p>0.05$).

Discussion

MASLD is a common liver disorder, affecting approximately 25.24 % of the global population, with a reported prevalence of about 29.81 % in China [3,15]. The pathogenesis of MASLD is complex and involves multiple mechanisms, including lipid accumulation, oxidative stress, and inflammation [16]. Recent studies have indicated that iron overload and ferroptosis are involved in the development of MASLD [17]. In this *in vitro* study, FFA treatment was observed to induce oxidative stress, iron overload, and ferroptosis in hepatocytes, and these changes were largely alleviated following liraglutide treatment.

Ferroptosis, an iron-dependent form of regulated cell death characterized by lipid peroxidation, has been previously identified in *in vivo* fatty liver models, including ob/ob mice and high-fat diet (HFD)-fed mice [18,14]. A study conducted by Yang *et al.* in HFD-treated $ApoE^{-/-}$ mice reported that, within liver tissue, expression of the iron transporter *TFR1* was upregulated, whereas the expression of ferroptosis-inhibitory genes *NRF2*, *SLC7A11*, and *GPX4* was suppressed [17]. Currently, *in vitro* data regarding ferroptosis in MASLD remain limited [17,19]. In this study, we found that FFA treatment enhanced cellular iron uptake through upregulation of *TFR1* and impaired the antioxidant defense system by downregulating *NRF2*, *SLC7A11*, and *GPX4,* resulting in increased oxidative stress and iron accumulation. Upregulation of *TFR1* suggests enhanced cellular iron uptake capacity, a key step in initiating ferroptosis. Conversely, downregulation of *NRF2* and its target GPX4 indicates impaired antioxidant defense, which increases susceptibility to lipid peroxidation and ferroptosis. These findings indicate that fatty acids can induce iron overload and ferroptosis in hepatocytes *in vitro*. Additionally, iron overload has been reported to promote fatty acid uptake and lipid accumulation in hepatocytes, while ferroptosis in hepatocytes may aggravate lipid accumulation, inflammation, and fibrosis by enhancing oxidative stress and lipid peroxidation [20-22]. Therefore, FFA-induced iron overload and ferroptosis may further exacerbate hepatocellular lipid accumulation and injury.

Liraglutide has been widely used in the management of T2DM and obesity. In recent years, beneficial effects of liraglutide on MASLD have been reported in both individuals with T2DM and T2DM-related animal models [23-28]. These effects are partially attributed to the alleviation of hepatocyte ferroptosis [13,14]. However, studies exploring the effects of liraglutide on MASLD in non-diabetic settings remain

limited. Liraglutide improves hepatic lipid markers in a hereditary hemochromatosis mouse model, and findings by Ji *et al.* demonstrated that liraglutide treatment improved liver function and reduced reactive oxygen species levels in HFD-fed mice [29,30]. Recent research by Chen *et al.* has provided novel insights into the therapeutic mechanisms of liraglutide in metabolic dysfunction-associated steatotic liver disease (MASLD) https://pubmed.ncbi.nlm.nih.gov/41377138/. These findings suggest that liraglutide ameliorates MASLD through a multi-pathway network involving ferroptosis inhibition, offering a systematic molecular basis for its clinical application in MASLD treatment https://pubmed.ncbi.nlm.nih.gov/41377138/[31].

Liraglutide may suppress ferroptosis through a dual mechanism: transcriptionally by reactivating the Nrf2/GPX4 axis to alleviate lipid peroxidation, and *via* GLP-1 receptor (GLP-1R)-mediated signaling. Activation of GLP-1R stimulates the PI3K/AKT pathway, which can inhibit GSK-3β through phosphorylation, thereby promoting Nrf2 nuclear translocation and upregulating downstream antioxidant genes, including GPX4 and HO-1 [32,33]. Similarly, a recent study in obese rats confirmed that liraglutide restored the SLC7A11/HO-1/GPX4 axis in a dose-dependent manner [34]. In this study, liraglutide alleviated oxidative stress and ferroptosis induced by FFA in hepatocytes *in vitro*. Prior studies have indicated that liraglutide can upregulate *NRF2* expression and enhance its activity in hepatocytes [12]. Consistently, our study showed that liraglutide treatment partially reversed the FFA-induced downregulation of NRF2 and GPX4, as well as the upregulation of TFR1.

Regarding SLC7A11, we observed that FFA significantly downregulated its expression, but liraglutide did not restore it. We speculate that SLC7A11 suppression in MASLD may be primarily driven by lipotoxicity rather than by GLP-1 receptor signaling. The inability of liraglutide to restore SLC7A11 may indicate that its anti-ferroptotic effects are mediated through SLC7A11-independent pathways, such as the Nrf2/GPX4 antioxidant axis, or that SLC7A11 represents a downstream target of lipotoxic injury that lies beyond the regulatory reach of GLP-1R activation. Therefore, the effects observed in this study may be associated with the ability of liraglutide to enhance cellular antioxidant defense mechanisms and regulate ferroptosis-related pathways.

Several limitations should be acknowledged. First, biochemical measurements (TG, GSH, SOD, MDA, and iron) were not normalized to total cellular protein content. Second, quantitative analysis of Oil Red O staining was not performed. Third, a GLP-1R antagonist was not used to confirm target specificity. Fourth, we did not perform NRF2 knockdown or GPX4 inhibition to confirm pathway dependency. Fifth, iron metabolism analysis focused only on TFR1, omitting ferritin and ferroportin. Sixth, the *in vitro* nature and use of HepG2 cells limit generalizability to *in vivo* pathophysiology. Seventh, full-length Western blot membranes with molecular weight markers were not retained at the time of experimentation due to limited documentation practices during the pandemic period. However, three independent replicates were performed with consistent results, and densitometric quantification is provided in Figure 5B. Future studies using *in vivo* models, primary hepatocytes, and mechanistic tools are needed.

Conclusions

Liraglutide improved cellular oxidative stress, iron overload, and ferroptosis induced by FFA in hepatocytes, which may contribute to its beneficial effects on MASLD.

Conflict of Interest

There is no conflict of interest.

Acknowledgements

This study was fund by Natural Science Foundation of Hebei Province (No. H2024206030). We thank the staff for their dedicated work in implementing the study's intervention and evaluation.

Abbreviations

ACSL4, Acyl-CoA synthetase long-chain family member 4; GPX4, Glutathione peroxidase 4; GSH, Glutathione; MASLD, Metabolic dysfunction-Associated Steatotic Liver Disease; MDA, Malondialdehyde; Nrf2, NFE2-related factor 2; SOD, Superoxide dismutase; SLC7A11, Heterodimeric protein containing a light chain; TFR1, Transferrin receptor 1.

References

1. Kazankov K, Jørgensen SMD, Thomsen KL, Møller HJ, Vilstrup H, George J, et al. The role of macrophages in nonalcoholic fatty liver disease and nonalcoholic steatohepatitis. Nat Rev Gastroenterol Hepatol 2019;16:145-159. https://doi.org/10.1038/s41575-018-0082-x
2. Yip TC, Lee HW, Chan WK, Wong GL, Wong VW. Asian perspective on NAFLD-associated HCC. J Hepatol 2022;76:726-734. https://doi.org/10.1016/j.jhep.2021.09.024
3. Ji J, Wu L, Wei J, Wu J, Guo C. The Gut Microbiome and Ferroptosis in MAFLD. J Clin Transl Hepatol 2023;11:174-187. https://doi.org/10.14218/JCTH.2022.00136
4. Feng G, Byrne CD, Targher G, Wang F, Zheng MH. Ferroptosis and metabolic dysfunction-associated fatty liver disease: Is there a link? Liver Int 2022;42:1496-1502. https://doi.org/10.1111/liv.15163
5. Younossi Z, Anstee QM, Marietti M, Hardy T, Henry L, Eslam M, et al. Global burden of NAFLD and NASH: trends, predictions, risk factors and prevention. Nat Rev Gastroenterol Hepatol 2018;15:11-20. https://doi.org/10.1038/nrgastro.2017.109
6. Yang WS, Stockwell BR. Ferroptosis: Death by lipid peroxidation. Trends Cell Biol 2016;26:165-176. https://doi.org/10.1016/j.tcb.2015.10.014
7. Yang Y, Chen J, Gao Q, Shan X, Wang J, Lv Z. Study on the attenuated effect of Ginkgolide B on ferroptosis in high fat diet induced nonalcoholic fatty liver disease. Toxicology 2020;445:152599. https://doi.org/10.1016/j.tox.2020.152599
8. Hayes JD, Dinkova-Kostova AT. The Nrf2 regulatory network provides an interface between redox and intermediary metabolism. Trends Biochem Sci 2014;39:199-218. https://doi.org/10.1016/j.tibs.2014.02.002
9. Valenti L, Fracanzani AL, Dongiovanni P, Rovida S, Rametta R, Fatta E, et al. A randomized trial of iron depletion in patients with nonalcoholic fatty liver disease and hyperferritinemia. World J Gastroenterol 2014;20:3002-3010. https://doi.org/10.3748/wjg.v20.i11.3002
10. Yan J, Yao B, Kuang H, Yang X, Huang Q, Hong T, et al. Liraglutide, Sitagliptin, and Insulin Glargine Added to Metformin: The Effect on Body Weight and Intrahepatic Lipid in Patients With Type 2 Diabetes Mellitus and Nonalcoholic Fatty Liver Disease. Hepatology 2019;69:2414-2426. https://doi.org/10.1002/hep.30320
11. Svegliati-Baroni G, Saccomanno S, Rychlicki C, Agostinelli L, De Minicis S, Candelaresi C, et al. Glucagon-like peptide-1 receptor activation stimulates hepatic lipid oxidation and restores hepatic signalling alteration induced by a high-fat diet in nonalcoholic steatohepatitis. Liver Int 2011;31:1285-1297. https://doi.org/10.1111/j.1478-3231.2011.02462.x
12. Zhu CG, Luo Y, Wang H, Li JY, Yang J, Liu YX, et al. Liraglutide Ameliorates Lipotoxicity-Induced Oxidative Stress by Activating the NRF2 Pathway in HepG2 Cells. Horm Metab Res 2020;52:532-539. https://doi.org/10.1055/a-1157-0166
13. Song JX, An JR, Chen Q, Yang XY, Jia CL, Xu S, Zhao YS, Ji ES. Liraglutide attenuates hepatic iron levels and ferroptosis in db/db mice. Bioengineered 2022;13:8334-8348. https://doi.org/10.1080/21655979.2022.2051858
14. Guo T, Yan W, Cui X, Liu N, Wei X, Sun Y, et al. Liraglutide attenuates type 2 diabetes mellitus-associated non-alcoholic fatty liver disease by activating AMPK/ACC signaling and inhibiting ferroptosis. Mol Med 2023;29:132. https://doi.org/10.1186/s10020-023-00721-7
15. Wang TY, George J, Zheng MH. Metabolic (dysfunction) associated fatty liver disease:more evidence and a bright future. Hepatobiliary Surg Nutr 2021;10:849-852. https://doi.org/10.21037/hbsn-21-352
16. Salvoza N, Giraudi PJ, Tiribelli C, Rosso N. Natural Compounds for Counteracting Nonalcoholic Fatty Liver Disease (NAFLD): Advantages and Limitations of the Suggested Candidates. Int J Mol Sci 2022;23:2764. https://doi.org/10.3390/ijms23052764
17. Yang Y, Chen J, Gao Q, Shan X, Wang J, Lv Z. Study on the attenuated effect of Ginkgolide B on ferroptosis in high fat diet induced nonalcoholic fatty liver disease. Toxicology 2020;445:152599. https://doi.org/10.1016/j.tox.2020.152599
18. An JR, Su JN, Sun GY, Wang QF, Fan YD, Jiang N, Yang YF, Shi Y. Liraglutide Alleviates Cognitive Deficit in db/db Mice: Involvement in Oxidative Stress, Iron Overload, and Ferroptosis. Neurochem Res 2022;47:279-294. https://doi.org/10.1007/s11064-021-03442-7

19. Liu H, Yan J, Guan F, Jin Z, Xie J, Wang C, Liu M, Liu J. Zeaxanthin prevents ferroptosis by promoting mitochondrial function and inhibiting the p53 pathway in free fatty acid-induced HepG2 cells. Biochim Biophys Acta Mol Cell Biol Lipids 2023;1868:159287. https://doi.org/10.1016/j.bbalip.2023.159287
20. Liang Y, Luo S, Bell S, Mo JMY, He B, Zhou Y, Bai X, Au Yeung SL. Do iron homeostasis biomarkers mediate the associations of liability to type 2 diabetes and glycemic traits in liver steatosis and cirrhosis: a two-step Mendelian randomization study. BMC Med 2024;22:270. https://doi.org/10.1186/s12916-024-03486-w
21. Qiu F, Wu L, Yang G, Zhang C, Liu X, Sun X, Chen X, Wang N. The role of iron metabolism in chronic diseases related to obesity. Mol Med 2022;28:130. https://doi.org/10.1186/s10020-022-00558-6
22. Stockwell BR, Friedmann Angeli JP, Bayir H, Bush AI, Conrad M, Dixon SJ, et al. Ferroptosis: A Regulated Cell Death Nexus Linking Metabolism, Redox Biology, and Disease. Cell 2017;171:273-285. https://doi.org/10.1016/j.cell.2017.09.021
23. Ying X, Rongjiong Z, Kahaer M, Chunhui J, Wulasihan M. Therapeutic efficacy of liraglutide versus metformin in modulating the gut microbiota for treating type 2 diabetes mellitus complicated with nonalcoholic fatty liver disease. Front Microbiol 2023;14:1088187. https://doi.org/10.3389/fmicb.2023.1088187
24. Honda J, Kimura T, Sakai S, Maruyama H, Tajiri K, Murakoshi N, Homma S, Miyauchi T, Aonuma K. The glucagon-like peptide-1 receptor agonist liraglutide improves hypoxia-induced pulmonary hypertension in mice partly via normalization of reduced ET(B) receptor expression. Physiol Res 2018;67(Suppl 1):S175-S184. https://doi.org/10.33549/physiolres.933822
25. Zhang L, Wu X, Li X, Chang X, Ding X, Wang Q, et al. Longitudinal changes in serum adropin levels and liver fat content during liraglutide treatment in newly diagnosed patients with type 2 diabetes mellitus and metabolic dysfunction-associated fatty liver disease. Acta Diabetol 2023;60:971-979. https://doi.org/10.1007/s00592-023-02082-3
26. Liao Z, Huang L, Chen J, Chen T, Kong D, Wei Q, et al. Liraglutide Improves Nonalcoholic Fatty Liver Disease in Diabetic Mice by Activating Autophagy Through AMPK/mTOR Signaling Pathway. Diabetes Metab Syndr Obes 2024;17:575-584. https://doi.org/10.2147/DMSO.S447182
27. Zhou R, Lin C, Cheng Y, Zhuo X, Li Q, Xu W, Zhao L, Yang L. Liraglutide Alleviates Hepatic Steatosis and Liver Injury in T2MD Rats via a GLP-1R Dependent AMPK Pathway. Front Pharmacol 2021;11:600175. https://doi.org/10.3389/fphar.2020.600175
28. Zhao X, Liu Y, Liu J, Qin J. Therapeutic Effects and Mechanism of Liraglutide in Rats with Type 2 Diabetes and Metabolic-associated Fatty Liver Disease. Endocr Metab Immune Disord Drug Targets 2022;22:963-969. https://doi.org/10.2174/1871530322666220126151141
29. Bozadjieva-Kramer N, Shin JH, Blok NB, Jain C, Das NK, Polex-Wolf J, et al. Liraglutide Impacts Iron Homeostasis in a Murine Model of Hereditary Hemochromatosis. Endocrinology 2024;165:bqae090. https://doi.org/10.1210/endocr/bqae090
30. Ji J, Feng M, Huang Y, Niu X. Liraglutide inhibits receptor for advanced glycation end products (RAGE)/reduced form of nicotinamide-adenine dinucleotide phosphate (NAPDH) signaling to ameliorate non-alcoholic fatty liver disease (NAFLD) in vivo and vitro. Bioengineered 2022;13:5091-5102. https://doi.org/10.1080/21655979.2022.2036902
31. Chen Y, Liu C, Yang Q, Yang J, Zhang H, Zhang Y, et al. Signatures of proteomics and glycoproteomics revealed liraglutide ameliorates MASLD by regulating specific metabolic homeostasis in mice. J Pharm Anal 2025;15:101273. https://doi.org/10.1016/j.jpha.2025.101273
32. Lu C, Xu C, Li S, Ni H, Yang J. Liraglutide and GLP-1(9-37) alleviated hepatic ischemia-reperfusion injury by inhibiting ferroptosis via GSK3β/Nrf2 pathway and SMAD159/Hepcidin/FTH pathway. Redox Biol 2025;79:103468. https://doi.org/10.1016/j.redox.2024.103468
33. Abdel Razek NS, Nassar NN, Sayed RH, El-Sahar AE, Abdallah DM. Liraglutide orchestrates ferroptosis defense against murine cisplatin acute kidney injury: NRF2 activation via both KEAP1-dependent and -independent mechanisms is essential for SLC7A11/GPX4 renoprotection. J Trace Elem Med Biol 2025;92:127755. https://doi.org/10.1016/j.jtemb.2025.127755
34. Song JX, An JR, Chen Q, Yang XY, Jia CL, Xu S, Zhao YS, Ji ES. Liraglutide attenuates hepatic iron levels and ferroptosis in db/db mice. Bioengineered 2022;13:8334-8348. https://doi.org/10.1080/21655979.2022.2051858